Determination of chromium speciation in natural waters by electrodeposition on graphite tubes for electrothermal atomization

ARTICLE *in* ANALYTICAL CHEMISTRY · SEPTEMBER 1980

Impact Factor: 5.64 · DOI: 10.1021/ac50061a007

2 AUTHORS, INCLUDING:

Graeme E Batley
Commonwealth Scientific and Industrial Res…

218 PUBLICATIONS **7,395** CITATIONS

SEE PROFILE

Co.: New York, 1945; p 251, 295, 326, 344, and 534.
(11) Hirschfeld, T.; Kizer, K. *Appl. Spectrosc.* **1975**, *29*, 345.
(12) Lynch, P. F.; Brady, M. M. *Anal. Chem.* **1978**, *50*, 1518.
(13) Liebman, S. A.; Alhstrom, P. H.; Griffiths, P. R. *Appl. Spectrosc.* **1976**, *30*, 355.
(14) Lephardt, J. O.; Fenner, R. A. *Appl. Spectrosc.* **1980**, *34*, 174.
(15) Koga, Y.; Sugie, M.; Kondo, S.; Saëki, S. *Bunseki Kagaku* **1979**, *28*, 298.
(16) Griffiths, P. R. "Fourier Transform Infrared Spectroscopy", Vol 1, Ferrero, J. R., Basile, L. J., Eds.; Academic Press: New York, 1978; p 143.
(17) Saperstein, D. D. U.S. Patent 4 182 926, 1980.
(18) Hanna, Alan; Marshall, John C.; Isenhour, T. L. *J. Chromatogr. Sci.* **1979**, *17*, 434, and references therein.
(19) Delaney, M. F.; Uden, P. C. *J. Chromatogr. Sci.* **1979**, *17*, 428.
(20) Hirschfeld, T. "Fourier Transform Infrared Spectroscopy", Vol 2, Ferraro, J. R., Basile, L. J., Eds.; Academic Press: New York, 1979; p 193.
(21) Elion, G. R.; Klink, A. E. U.S. Patent 4 055 511, 1977.
(22) Nagy, J. B.; Gilsen, J. P.; Derouane, J. *J. Mol. Catal.* **1979**, *5*, 393 and references therein.
(23) Ferraro, J. R.; Basile, L. J. "Fourier Transform Infrared Spectroscopy", Vol 1, Academic Press: New York, 1978; p 283, Figure 5.
(24) Carberry, J. J. "Chemical and Catalytic Reaction Engineering", McGraw-Hill: New York, 1976.
(25) Mills, G. A.; Steffgen, F. W. *Catal. Rev.* **1973**, *8*, 159.
(26) Inui, T.; Funabiki, M.; Suehiro, M.; Sezune, T.; Iwana, T. *Nippon Kagaku Kaishi* **1978**, *4*, 517.
(27) Colthup, N. B.; Daly, L. H.; Wiberly, S. E. "Introduction to Infrared and Raman Spectroscopy"; Academic Press: New York, 1964; Chapter 5, p 364.
(28) Kurganova, S. Y.; Rudenko, A. P.; Balandin, A. A. *Zh. Org. Khim.* **1966**, *2*, 804.
(29) McAllister, S. H.; Bailey, W. A.; Bolton, C. M. *J. Am. Chem. Soc.* **1940**, *62*, 3211.
(30) Scheidt, F. M. *J. Catal.* **1964**, *3*, 372.
(31) Tada, A. *Bull. Chem. Soc. Jpn.* **1975**, *48*, 1391.
(32) Pouchert, C. J., Ed., "The Aldrich Library of Infrared Spectra"; Aldrich Chemical Co: Milwaukee, Wis., 1970.
(33) Vandef, A.; Bouche, R. *Spectrosc. Lett.* **1979**, *12*, 371.

RECEIVED for review February 6, 1980. Accepted June 2, 1980.

Determination of Chromium Speciation in Natural Waters by Electrodeposition on Graphite Tubes for Electrothermal Atomization

Graeme E. Batley*

Analytical Chemistry Section, Australian Atomic Energy Commission, Lucas Heights, N.S.W., 2234 Australia

Jaroslav P. Matousek

Department of Analytical Chemistry, University of New South Wales, P.O. Box 1, Kensington, N.S.W., 2033 Australia

An analytical technique has been developed for the study of chromium speciation in natural waters based on the atomization of electrodeposited species. Matrix interferences can be overcome and preconcentration achieved by the electrodeposition of chromium with mercury, onto pyrolytic graphite-coated tubular furnaces, using a flow-through assembly. At pH 4.7, using a deposition potential of −1.8 V vs. SCE, both Cr(VI) and Cr(III) are reduced and accumulated as metallic chromium. At the same pH, but at −0.3 V vs. SCE, only Cr(VI) is selectively reduced to Cr(III) which accumulates by adsorption. Using the labile-bound discrimination of the electrodeposition technique combined with an ultraviolet irradiation step, Cr(VI) was found to be dominant in the samples studied, with most Cr(VI) present as labile forms.

Because of the difference in toxicity of hexavalent and trivalent chromium to aquatic biota, there have been many attempts in recent years to discriminate between species in these two oxidation states in natural waters (*1*). Trivalent chromium is recognized as essential to mammals for the maintenance of an effective glucose, lipid, and protein metabolism. In the hexavalent state, however, chromium can diffuse, as CrO_4^{2-}, through cell membranes, when it can oxidize and bind to other important biological molecules with toxic results.

Most of the early studies of chromium speciation (*2–6*) relied upon the ability of ferric hydroxide to selectively coprecipitate Cr(III) (*2, 3*), with Cr(VI) being determined after reduction, usually using SO_2. Selective solvent extraction of Cr(VI) from seawater was reported by De Jong and Brinkman (*7*). Chromium(VI) was quantitatively extracted by Aliquat-336 from weakly acidic (pH 2) samples, while Cr(III) was extracted after oxidation by ammonium persulfate. More recently, ion-exchange separations have been investigated (*8*) and these form the basis of a field technique proposed by Shuman and Dempsey (*9*). It is not possible, however, to equate anion-exchangeable chromium with Cr(VI) species or cation-exchangeable chromium with Cr(III), since $Cr(OH)_4^-$, predicted to be the dominant form of Cr(III) in seawater (*5, 10*), will be retained in the anion-exchangeable fraction. The nonexchangeable fraction will consist of neutral polymeric species or chromium adsorbed or occluded in colloidal species and unable to penetrate the resin pore network.

Inherent in all these procedures is the need to separate the metal species before analysis from the sodium chloride matrix, since it can interfere in any direct atomic absorption measurements. We have shown previously (*11*) that the separation and preconcentration of cobalt and nickel species from seawater can be readily achieved by their electrodeposition, in the presence of added mercuric ions, onto a graphite tube prior to the atomization of the deposited metals. This paper describes further studies of the electrodeposition–atomization technique and examines its potential for the analysis of chromium species in seawater.

EXPERIMENTAL

Apparatus. Electrodepositions were carried out using a Princeton Applied Research model 174 polarographic analyzer, and the cell assembly is shown in Figure 1. The cell, constructed from Perspex, consisted of a threaded top section containing the three electrodes and gas inlet tubes and a detachable base section capable of holding 25 mL of solution. Pyrolytic graphite-coated tubes (9 mm × 3 mm i.d.) supplied by Ultra Carbon Corp., Bay City, Mich., were used as replaceable cathodes. For experiments on deposit distributions, tubes supplied by Varian Techtron were also used. A tube was held by a polythene screw in the recessed end of the Teflon tube. Pressure contact was made with the end of the graphite electrode, by a platinum wire inserted through a separate hole in the Teflon tube. The pyrolytic graphite coating was scraped from the upper end of the electrode to ensure good electrical contact. During electrolysis, the graphite cathode should be fully covered by solution. The anode consisted of a coil of platinum wire. A ceramic plug salt bridge was used to connect a Beckman No. 39178 fibre-junction, saturated calomel electrode (SCE). Nitrogen flow could be regulated either above or under the solution via Pyrex glass inlet tubes.

Solution was circulated through the cathode and returned to the cell at 2.2 mL s^{-1} using a Masterflex pump drive (model 7544-80) and head (model 7015-20).

0003-2700/80/0352-1570$01.00/0

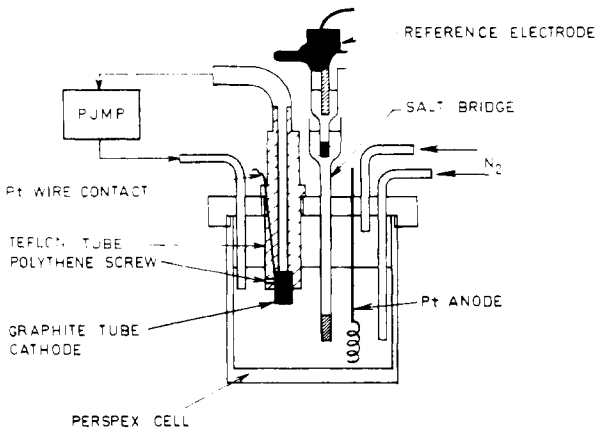

Figure 1. Cell assembly

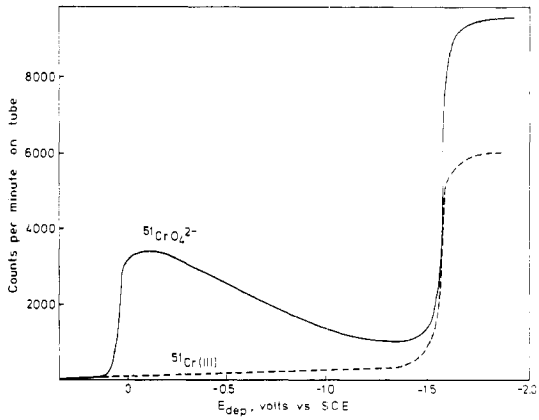

Figure 2. Effect of potential on the deposition of $^{51}CrO_4^{2-}$ and $^{51}Cr(III)$; 0.5 M NaCl, 0.016 M acetate, pH 4.7, 1.8×10^{-4} M $Hg(NO_3)_2$

Atomic absorption analyses were performed on a Varian Techtron AA-5 spectrometer using the CRA-90 furnace accessory. A Varian Techtron chromium hollow cathode lamp was operated at 8 mA, and the 357.9-nm line monitored, using the power supply in the atomization mode with a programmed ramp at 500 °C s^{-1}, to 2200 °C with 2-s hold. Peak heights were recorded on a Mace FBQ100 chart recorder. To examine atomization behavior, a fast detection system (time constant, 2 ms) was used to record signal profiles. The signal from the photomultiplier was led directly to the input of a Biomation model 805 waveform recorder which was triggered by the furnace power supply when it commenced the atomization stage. Recorded signals were displayed on a Tektronix 7504 oscilloscope and plotted using the slow analogue output of the waveform recorder.

Furnace temperatures were measured using an Ircon series 6000 radiation thermometer (Ircon Inc., Skokie, Ill.) with the temperature range of 1000 to 3000 °C. Radiation from the central inner area of the furnace was monitored and the output of the radiation thermometer was fed directly into the waveform recorder.

Reagents. Merck Suprapur grade reagents were used throughout. Tracer solutions of chromic chloride (^{51}Cr) and sodium chromate (^{51}Cr) were supplied by the Isotope Division, Australian Atomic Energy Commission.

Water samples were collected in acid-washed high density polythene bottles as described previously (*12*). After filtration through a 0.45-μm membrane filter, samples were stored at 4 °C until analyzed.

Procedure. Clean the cell and associated circulation system, before use, with dilute nitric acid, followed by distilled water. To a 25-mL volumetric flask, add 0.2 mL of 2 M acetate buffer pH 4.7 and 0.3 mL of 1.5×10^{-2} M $Hg(NO_3)_2$ and make up to volume with sample. Transfer the solution to the cell base. With Teflon-tipped tweezers, place a graphite tube in the cathode holder and tighten the holding screw using an acid-cleaned Perspex screwdriver. Position the cathode holder, activate the pumping system, and deaerate the solution with nitrogen for 5 min. Preset the deposition potential, and with gas now passing over the solution, commence the electrodeposition for the required time. At the completion of this period, unscrew the cell base, allowing the pump tubing to empty, and then quickly hold in position a second cell base filled with distilled water. Allow several seconds for water to be drawn through the cathode tube, remove the cell base, and withdraw the cathode holder. Remove excess water from the outside face of the graphite tube with a filter paper. Unscrew the polythene screw, remove the graphite tube using the Teflon-coated tweezers, and turn off the applied voltage and pumping system. Position the tube on a watch glass under an infrared lamp to dry for several minutes and then place in a pill-pack until ready to measure. For measurement, transfer the tube to the graphite furnace atomizer unit of the atomic absorption spectrometer.

RESULTS AND DISCUSSION

Electrodeposition of Chromium. The selection of suitable electrodeposition potentials was made by studying the deposition with mercury of both $^{51}CrO_4^{2-}$ and $^{51}Cr^{3+}$ over a wide potential range. The activity of the deposit as a function of deposition potential is plotted in Figure 2. At pH 4.7, the reduction of CrO_4^{2-} gave rise to a peak at −0.3 V vs. SCE, which is consistent with the first polarographic peak reported by Issa et al. (*13*). It is significant that, at more negative potentials, no accumulation occurred, the product being completely reduced to a soluble Cr(III) species which was desorbed as a result of the negative charge assumed by the electrode. In more alkaline solution (pH 8.6), this peak was shifted to −0.5 V vs. SCE but was absent from solutions acidified to below pH 2. The plots in Figure 2, for both Cr(III) and CrO_4^{2-}, show steps at −1.6 V vs. SCE, consistent with the polarographic wave for reduction to metallic chromium.

The polarographic reduction of chromium has been studied by a number of workers (*13–15*). In unbuffered KCl solution, the reduction of chromate ion gives rise to four polarographic waves at −0.3, −1.0, −1.6, and −1.8 V vs. SCE, respectively, the latter three being attributed to reductions to Cr(III), Cr(II) and Cr(0), respectively (*14*). In solutions buffered between pH 4 and 6.5, two waves are observed at −0.3 and −1.6 V vs. SCE, respectively. Again the latter wave is due to reduction to Cr(0) (*13*).

The first wave is characterized by a large maximum and the electrode reactions giving rise to it have been the subject of some debate. The reduction has been shown to be adsorption-controlled, with the adsorbed species being Cr(VI) (*13*). Lingane and Kolthoff (*14*) attributed these waves to the formation at the electrode of a film of either chromium(III) hydroxide or a basic chromic chromate, which inhibits the complete reduction of CrO_4^{2-} to Cr(III).

The stripping voltammetry of this primary chromate reduction product at a graphite electrode has been examined by Krapivkina and Brainina (*16*). A linear dependence of anodic current on chromate concentration was observed for the stripping of accumulated $Cr(OH)_3$. Deposition at −0.5 V vs. SCE from a solution at pH 4.7 gave a stripping peak at +0.9 V. At this pH, a detection limit of 0.1 mg L^{-1} was reported, although a higher sensitivity was achievable in ammonia buffer. This sensitivity is governed by the reversibility of the reduction and by the presence of interfering waves such as the oxidation of chloride ion in seawater.

Fuoco and Papoff (*17*) claimed the ability to resolve Cr(VI) and Cr(III) by differential pulse polarography in ammonia buffer, with a detection limit of 2.6 μg L^{-1}. Copper, however, interfered with the analysis. Using stripping voltammetry at a hanging mercury drop (HMDE) at pH 9.6, they were able to detect as little as 1.6 μg L^{-1} total chromium. Accumulation was carried out at −1.40 V vs. SCE, and the stripping peak obtained at −1.31 V was assumed to be due to the oxidation of deposited $Cr(OH)_2$.

As we have shown previously (*11*), the use of the graphite tube electrode with in-situ mercury deposition is superior to

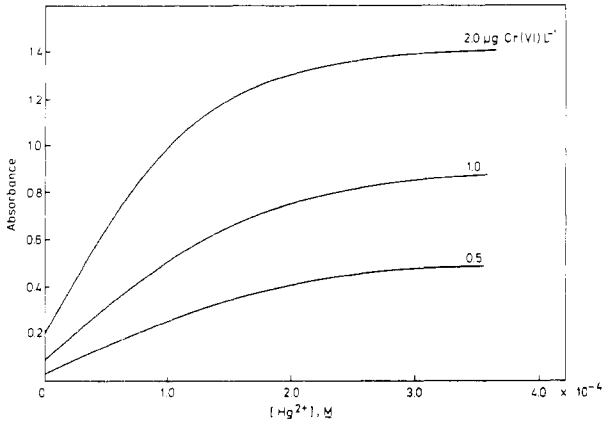

Figure 3. Effect of Hg^{2+} concentration on the absorbance for electrodeposits from CrO_4^{2-} solutions; 0.5 M NaCl, 0.016 M acetate, pH 4.7

the HMDE, especially at extreme cathodic potentials where hydrogen evolution can dislodge the drop. Where film formation occurs, the HMDE is again inferior, its area being only 4.5% of that for the graphite tube, and measurements using radiotracers showed that it was possible to accumulate a greater amount of chromium than at the HMDE. The effect of solution mercury concentration on the amount of chromium deposited is shown in Figure 3. Theoretically, as shown by the Roe and Toni equation (*18*), the amount of a metal deposited, measured by its stripping current, should be independent of mercury concentration, once a mercury film has been established. This equation, however, assumes the metal to be soluble in the mercury film. The observed behavior is the result of mercury droplets, as they are deposited, being rapidly coated with the insoluble chromium reduction product. A limiting concentration is reached beyond which film formation prevents a further increase in electrode area. For higher concentrations, surface saturation occurs at lower solution mercury concentrations.

A mercuric ion concentration in the solution of 1.8×10^{-4} M was chosen for routine analyses. For this value, a linear relationship between solution Cr(VI) concentration and measured absorbance was obeyed for chromium concentrations up to 6 $\mu g\ L^{-1}$ and deposition times of six minutes (Figure 4a). There was a small yet significant deposition of Cr(III) at −0.3 V, amounting to less than 10% of the Cr(VI) deposited for the same solution concentration. This presumably arises from weak adsorption of Cr(III) at the electrode surface.

At −1.8 V vs. SCE, both Cr(VI) and Cr(III) are deposited, with the slope of the absorbance vs. concentration plot for Cr(VI) being 1.74 times that for Cr(III), owing to differences in the diffusion coefficients of the two species (Figure 4b). The equation derived by Blaedel et al. (*19*), for the diffusion controlled electrolysis current at constant flow through a tubular electrode, predicts a dependence on $D^{2/3}$, where D is the diffusion coefficient of the reducible species. Diffusion coefficients determined polarographically for CrO_4^{2-} and Cr(III) in 0.5 M NaCl buffered to pH 4.7 were 2.48 and 1.05 $\times 10^{-5}$ $cm^2\ s^{-1}$, respectively. The ratio $(D_{CrO_4^{2-}}/D_{Cr(III)})^{2/3}$ of 1.77 is therefore consistent with the observed differences in slopes for the two calibration plots.

Depositions at both −0.3 V and −1.8 V were shown to give linear relationships between measured absorbances and deposition times. For a concentration of 1 $\mu g\ L^{-1}$ Cr, these relationships were linear for deposition times up to 12 min. With longer deposition times, the amount of chromium deposited lies outside the linear working range of the atomic absorption method. Using these deposition times, the electrolysis is, of course, not exhaustive. Calculations indicated that less that 1% of an available chromium concentration of

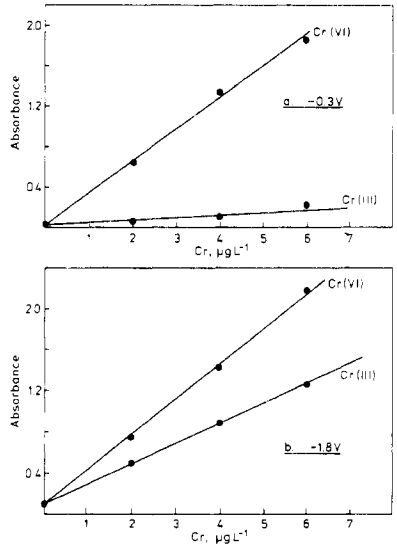

Figure 4. Calibration plots for the deposition of Cr(VI) and Cr(III); (a) −0.3 V vs. SCE, (b) −1.8 V vs. SCE; 0.5 M NaCl, 0.016 M acetate, pH 4.7, 1.8×10^{-4} M $Hg(NO_3)_2$

1 $\mu g\ L^{-1}$ was deposited during a 6-min electrolysis.

Distribution of Deposited Metal. Using the cell illustrated in Figure 1, it was expected that, in the presence of an applied voltage, the current density distribution along the tubular electrode would be nonuniform. With solution being drawn from the solution end through to the holder end, the current density should be greatest at the lower end, diminishing to the top. During electrolysis, deposition will occur on both the inner and outer faces of the tube. However, provided the same proportion of metal is deposited in this region, it can be assumed that there will be no error involved in measuring by atomization only the metal on the internal surface. This latter amount must necessarily be greater than that on the external surface, where the efficiency of mass transport is poor due to inefficient stirring.

The distribution of deposit on the internal tube surfaces was studied using $^{51}Cr(III)$. After deposition, approximately 1-mm sections were successively abraded from the end of a tube using a fine glass paper, and the remaining portion was counted using a well γ-counter with NaI crystal detector. The distribution curves obtained in this manner, for different electrode and flow arrangements, are illustrated in Figure 5. In each case, a significant deposit accumulated on the end face; however, experiments showed that this did not contribute significantly to the atomization signal. In the absence of an injection hole in the tube (Ultra Carbon tubes) as shown in Figure 5a, the deposit distribution was decidedly asymmetric with the largest fraction on the lower end. For a tube having a central injection hole through which sample could also enter (Varian tube, Figure 5b), the effect was an increased deposit in the center section. If the solution flow was reversed, a more uniform deposit was achieved, although it was still greater at both ends (Figure 5c). This flow pattern is undesirable since, at the time of removal of the cell, solution continues to pump through the electrode with the applied voltage disconnected, with the possibility of washing away a portion of the deposit. With flow in the opposite direction, this does not occur since the electrode remains free of solution at the instant of removal of the applied voltage.

Ideally, the highest sensitivity is expected with the analyte element concentrated in the center of the furnace. If the metal is deposited near the ends of the tube, it is subjected to higher diffusion losses and also to a slower rate of atomization. In an attempt to achieve a more favorable distribution, a second platinum anode was introduced into the Teflon holder

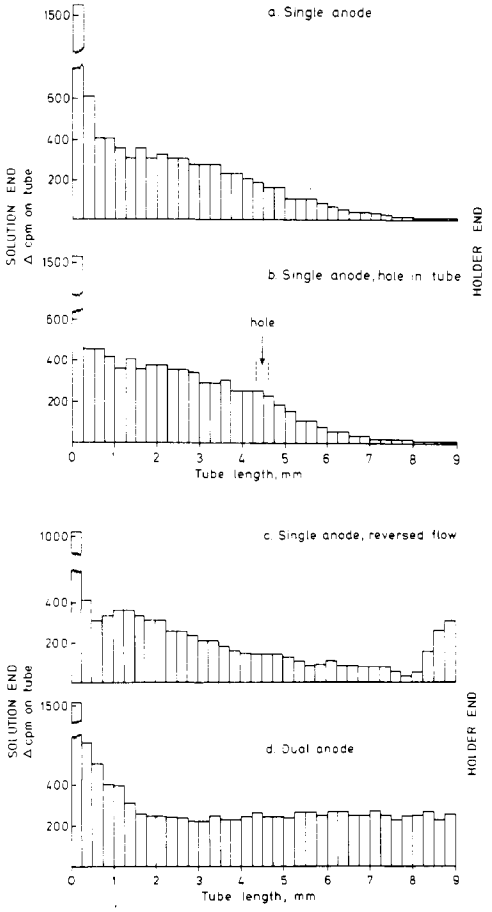

Figure 5. Distribution of deposits from $^{51}CrO_4^{2-}$ solutions for different electrode configurations; 0.5 M NaCl, 0.016 M acetate, pH 4.7, 1.8 × 10^{-4} M $Hg(NO_3)_2$

downstream of the cathode. Figure 5d shows that the distribution achieved in this manner was improved over the previous examples. Even in this instance, an appreciable portion of the deposit remained at the ends of the tube, and experiments showed that there was only marginal improvement in sensitivity over the distribution obtained using a single anode.

Atomization Characteristics. Despite the separation achieved in the electrodeposition step, traces of saline matrix adhered to the surface of the furnace. During the atomization stage, these gave rise to a molecular background signal of variable magnitude. With the atomization ramp rate of 500 °C s^{-1}, this preceded the atomic absorption signal and was well resolved using both the fast and the conventional detection systems.

During electrodeposition, chromium is accumulated as metal or $Cr(OH)_3$, depending on the selected reduction potential. In the atomization step, the different chemical forms of chromium should, in general, require different temperatures for their conversion to gaseous atoms. This behavior can be characterized by measuring peak atomization temperatures (*20*). Fast, time-resolved absorption and temperature measurements were used to generate data shown in Figure 6. For the electrodeposited species, the peak atomization temperatures follow the expected trend, with metallic chromium being atomized at a lower temperature than the oxygen containing compound. For a given chemical form, the peak atomization temperature should be constant (*20*); however, the slight variation observed in Figure 6 reflects in part variation in the deposit distribution.

When CrO_4^{2-} solution was injected into the furnace, resulting in most of the sample being concentrated in the central

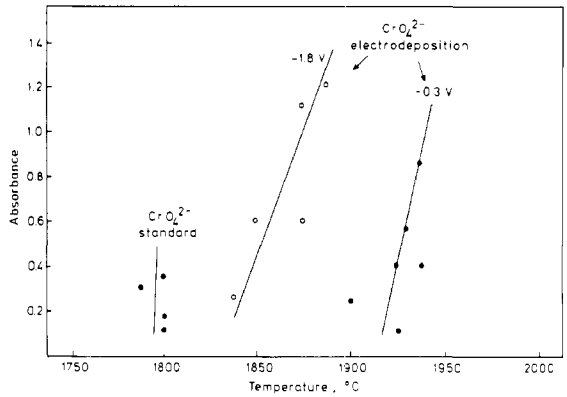

Figure 6. Peak atomization temperatures for standard CrO_4^{2-} solutions, deposited Cr metal (−1.8 V), and deposited $Cr(OH)_3$ (−0.3 V). The temperature scale refers to the maximum wall temperature

Table I. Chromium Species in Saline Waters, μg L^{-1}

source of sample	salinity, ‰	labile Cr(VI)	labile Cr(III)	total Cr
Cronulla Point, Australia	35	0.13	0.08	0.25
Woronora River, Australia	21	0.20	0.03	0.31
Georges River, Australia	35	0.68	0.22	1.25

furnace area, the measured peak atomization temperature appeared to be significantly lower than that for the electrodeposited oxidized form of chromium. In this instance, apart from the chemical form, the different sample distribution affected the measured value. While quantitative evaluation is difficult owing to the complexity of the time-dependent supply and removal functions (*21*), this behavior can be rationalized by considering the temperature gradient present along the furnace during the atomization step. For the atomization parameters used, the furnace end temperature and the average furnace temperature lagged behind the maximum wall temperature, which is plotted in Figure 6, by approximately 150 and 70 °C, respectively (*22*). Portions of the analyte element deposited on the cooler parts of the furnace therefore appeared later or at apparently higher atomization temperatures when plotted against the maximum furnace temperature.

Chromium in Seawater. The practical utility of the electrodeposition technique was tested by the analysis of chromium species in a number of saline water samples. Absorbances for chromium deposited at −0.3 V and −1.8 V, from samples buffered to pH 4.7, were calibrated by the method of standard additions. This permitted calculation of the concentrations of labile Cr(VI) and Cr(III), respectively. Implicit in these calculations is the assumption that the concentrations of labile Cr(VI) are equal at the two deposition potentials. This is not unreasonable since the existence of any complexed Cr(VI) species is unlikely. The only species likely to be in a bound form will be the small fraction adsorbed on colloidal matter, which is assumed to behave similarly at both potentials.

The determination of total chromium requires a more vigorous treatment than the boiling of an acidified sample used for other bound heavy metals in seawater, since the dissociation of inert Cr(III) complexes is slow. Experiments with UV irradiation of seawater in the presence of hydrogen peroxide showed that after a 6-h irradiation of an acidified sample, all Cr(VI) species had been reduced to Cr(III) with all organic matter being fully decomposed. The completeness of this reduction was confirmed by measurements at −0.3 V.

Results for the analysis of some saline water samples are shown in Table I. Previously published results for chromium in both seawater and river water have been summarized by Florence and Batley (*1*). In seawater, typical Cr(VI) concentrations lie in the range 0.1–1.3 $\mu g\ L^{-1}$ with Cr(III) from 0.002–0.05 $\mu g\ L^{-1}$. The lowest concentrations are found in open ocean waters. In keeping with theoretical predictions (*5*), Cr(VI) is usually dominant. The redox equilibrium between Cr(III) and Cr(VI) is, however, a function of oxygen content and the amount of colloidal and particulate matter, both organic and inorganic. In near-shore and river waters, changes in these parameters result in a general lowering of Cr(VI)/Cr(III) ratios. The results in Table I confirm this finding. It is likely, for these samples, that most of the Cr(VI) is present in labile forms while Cr(III) is distributed between both bound and labile forms.

Although a more detailed speciation study is not reported here, experiments have shown that this would be possible using an anion-exchange resin to remove the anionic species $Cr(OH)_4^-$, $HCrO_4^-$, and CrO_4^{2-}.

Blank chromium values for added reagents were found to be negligible. Tube blanks were equivalent to less than 0.02 absorbance unit. The limit of detection using a 15-min deposition was 0.05 μg Cr L^{-1}. A typical relative standard deviation calculated from replicate measurements of 0.4 μg Cr(VI) L^{-1} was 13%.

LITERATURE CITED

(1) Florence, T. M.; Batley, G. E. *C.R.C. Crit. Rev. Anal. Chem.* **1980**, in press.
(2) Cutshall, N.; Johnson, V.; Osterberg, C. *Science* **1966**, *152*, 202–203.
(3) Chuecas, L.; Riley, J. P. *Anal. Chim. Acta* **1966**, *35*, 240–246.
(4) Fukai, R.; Vas, D. *J. Oceanogr. Soc. Jpn.* **1967**, *23*, 298–305.
(5) Elderfield, H. *Earth Planet. Sci. Lett.* **1970**, *9*, 10–16.
(6) Cranston, R. E.; Murray, J. W. *Anal. Chim. Acta* **1978**, *99*, 275–282.
(7) De Jong, G. J.; Brinkman, U. A. Th. *Anal. Chim. Acta* **1978** *98*, 243–250.
(8) Pankow, J. F.; Leta, D. P.; Lin, J. W.; Ohl, S.E.; Shum, W. P.; Janauer, G. E. *Sci. Total Environ.* **1977**, *7*, 17–26.
(9) Shuman, M. S.; Dempsey, J. H. *J. Water Pollut. Control Fed.* **1977**, *49*, 2000–2006.
(10) Sibley, T. H.; Morgan, J. J. *Proc. Int. Conf. Heavy Metals Environ.* **1975**, *1*, 319–338.
(11) Batley, G. E.; Matousek, J. P. *Anal. Chem.* **1977**, *49*, 2031–2035.
(12) Batley, G. E.; Gardner, D. *Water Res.* **1977**, *11*, 745–756.
(13) Issa, R. M.; Abd-el-Nabey, B. A.; Sadek, H. *Electrochim. Acta* **1968**, *13*, 1827–1836.
(14) Lingane, J. J.; Kolthoff, I. M. *J. Am. Chem. Soc.* **1940**, *62*, 852–858.
(15) Green, J. H.; Walkley, A. *Aust. J. Chem.* **1955**, *8*, 51–61.
(16) Krapivkina, T. A.; Brainina, Kh. Z. *Zavod, Lab.* **1967**, *33*, 400–402.
(17) Fuoco, R.; Papoff, P. *Ann. Chim. (Rome)* **1975**, *65*, 155–163.
(18) Roe, D. K.; Toni, J. E. A. *Anal. Chem.* **1965**, *37*, 1503–1506.
(19) Blaedel, W. J.; Klatt, L. N. *Anal. Chem.* **1966**, *38*, 879–883.
(20) Czobik, E. J.; Matousek, J. P. *Talanta* **1977**, *24*, 573–577.
(21) van den Broek, W. M. G. T.; de Galan, L. *Anal. Chem.* **1977**, *49*, 2176–2186.
(22) van den Broek, W. M. G. T.; de Galan, L.; Matousek, J. P.; Czobik, E. J. *Anal. Chim. Acta* **1978**, *100*, 121–138.

RECEIVED for review February 1, 1980. Accepted May 30, 1980.

Organic Matrix Modifiers for Direct Graphite Furnace Atomic Absorption Determination of Cadmium in Seawater

Roger Guevremont

Atlantic Regional Laboratory, National Research Council of Canada, 1411 Oxford Street, Halifax, Nova Scotia, Canada, B3H 3Z1

EDTA, citric acid, histidine, lactic acid, and aspartic acid are effective matrix modifiers for direct graphite furnace analysis of seawater. The addition of less than 1 mg mL^{-1} to undiluted seawater promotes low temperature atomization of cadmium, and significantly reduces interference from the volatilization of other matrix components. Citric acid provided the highest sensitivity in both distilled water and seawater. Lower limits of analysis of 0.01 μg Cd L^{-1} and a precision of ±7% at 0.07 μg Cd L^{-1} in seawater were obtained with aspartic acid.

Considerable effort has been directed to the development of rapid and reliable methods for the analysis of trace metals in seawater. Quite aside from the major problems of contamination and losses during sampling and storage of seawater, the high salt content of the matrix and the very low concentrations of trace metals contribute considerable difficulty to the analysis. The most widely used methods include a preconcentration step which serves to remove the bulk of the matrix and to increase the concentration of metals to a level where a reliable measurement may be made. Included among these are solvent extraction (*1*, *2*), chelating ion exchange (*2–4*), coprecipitation (*5*), and electrochemical reduction (*6*). The concentrate may be analyzed by a variety of instrumental techniques including neutron activation (*7*, *8*), optical emission spectrometry, mass spectrometry (*2*), and flame and flameless atomic absorption spectrometry (*2*, *3*).

Graphite furnace atomic absorption analysis is one of the few instrumental techniques which has the sensitivity needed to measure trace elements in seawater without a preconcentration step. However, the matrix introduces significant background absorbance problems since most elements are covolatilized with the bulk of the matrix. As a result many workers report limited success with direct methods (*3*, *9*, *10*).

The addition of matrix modifiers to seawater has led to successful analysis of several elements by direct graphite furnace atomic absorption measurement. Useful modifiers include NH_4NO_3 (*11*, *12*), $(NH_4)_2S_2O_8$ (*13*), HNO_3 (*14*) and ascorbic acid (*15*). Further developments of direct methods of seawater analysis should have great potential to reduce the time required for analysis, reduce possible sources of contamination, and simplify the measurement of the analytical blank. Automation of the analysis also becomes possible.

An earlier publication (*16*) described the application of EDTA to direct graphite furnace atomic absorption analysis of seawater. EDTA is the first compound reported which is capable of promoting efficient low temperature atomization of cadmium from the salt matrix. In the presence of such a matrix modifier, or releasing agent, the atomic absorption signal due to cadmium appears free of the background interference caused by volatilization of the bulk of the seawater

0003-2700/80/0352-1574$01.00/0